From Nonlinear System Analysis and Synthesis: Vol. 2 - Techniques and Applications, published by the ASME, Feb. 1981.

Part 2, Chapter 7

# COVARIANCE ANALYSIS OF NONLINEAR SIOCHASIIC SYSTEMS VIA SIATISIICAL LINEARIZATION

James H. Taylor

School of Mechanical and Aerospace Engineering
Oklahoma State University
Stillwater, Oklahoma 74078

and

Charles F. Price, Joseph Siegel, and Arthur Gelb

The Analytic Sciences Corporation
Reading, Massachusetts 01867

Abstract. Covariance analysis can be combined with describing function theory (statistical linearization) to provide a method for the direct statistical analysis of nonlinear stochastic systems. It combines the efficiency of covariance analysis with the realism of quasi-linear describing functions in capturing the amplitude dependence of signal transfer through nonlinear devices. Ihis paper presents the basic principles of this approach and summarizes a variety of problems that have been treated successfully with the technique.

## 1. INIRODUCTION

In the past, the only feasible method of analyzing the statistical performance of a nonlinear dynamic system driven by random inputs has been the use of monte carlo simulation. However, associated with the monte carlo method is the problem of obtaining a sufficiently large sample size (number of simulation trials) to provide the required confidence in the results[1]. Because of the expense and time required to perform many monte carlo trials -- often 200 or more are needed -- the monte carlo method is not a very satisfactory tool for performing sensitivity and parameter tradeoff studies, since an entirely new set of simulations must be generated each time a variable is changed.

Linear covariance analysis [2] is a mathematical technique which yields the exact second-order ensemble statistics (means and variances) for linear system variables as functions of time. Therefore, a single solution of the system covariance equations directly provides the desired results. Ihis generally requires substantially less computer time than a large ensemble of monte carlo trials. However, covariance analysis -- in the usual sense -- can only be applied to linear or linearized systems.

[1] Ihe problem of choosing an appropriate sample size is addressed in [1].

The most common technique used to deal with a nonlinear system is small-signal linearization, in which each nonlinearity is expanded in a Taylor series about some operating point -- i.e., a nominal trajectory -- and only the linear terms of the expansion are retained. This approximates the nonlinearity only for "small" perturbations about the operating point. Furthermore, there are many important nonlinear relationships which exhibit discontinuities (e.g., limiters, quantizers, and dead zones) for which the required partial derivatives do not exist; this is a major restriction which limits the applicability of Taylor series linearization.

A more powerful approach is statistical linearization, in which a nonlinear operation is approximated by a linear one that represents the transfer characteristic of the nonlinearity and depends on some properties of the input signal, namely, form and amplitude. This procedure, often referred to as quasi-linearization, results in different linear approximations to the same nonlinearity for different assumed input signal forms, with the associated "gains" dependent upon input signal amplitude. Quasi-linear approximators of this type are termed describing functions and have received extensive treatment in [3, 4, 5, 6, and 7]. Using statistical linearization, the assumed form for signals in systems having stochastic inputs is restricted to a bias plus a zero-mean gaussian random process; the input signal level or amplitude is measured in terms of its mean (bias level) and the standard deviation of the random process. Because the quasi-linear model that results depends upon the nonlinearity input signal statistics, any range of input signal magnitude can be accommodated realistically.

The application of covariance analysis to stochastic system models containing quasi-linear approximators for nonlinear effects has proven to be very effective. This approach, called the Covariance Analysis Describing Function Technique (CADET[TM]), was first independently proposed in [6,8] and has been developed more fully in [9-11]. Additional detail on the theory of CADET is provided in Appendices A and B. The main body of the paper presents examples of a few specific nonlinear systems which have been successfully analyzed with the technique.

## 2. APPLICATIONS

Three examples of the application of CADET are discussed in this section. The first, concerning an antenna pointing and tracking study, is treated in some detail, to illustrate the CADET methodology. The next example is a simple pursuer/evader intercept problem, and the third is a spacecraft spin-up study.

### 2.1 ANTENNA POINTING AND TRACKING PROBLEM

The function of the antenna pointing and tracking system modeled in Fig. 1 is to follow a target line-of-sight (LOS) angle, $\theta_t$. Assume that $\theta_t$ is a deterministic ramp,

$$\dot{\theta}_t = \omega u_{-1}(t) \tag{1}$$

where $\omega$ is the slope of the ramp and $u_{-1}$ denotes the unit step function. The pointing error,

---

The term CADET is a trademark of The Analytic Sciences Corporation.

$$e = \theta_t - \theta_a \tag{2}$$

where $\theta_a$ is the antenna centerline angle, is the input to a nonlinearity $f(\cdot)$ which represents the limited beamwidth of the antenna; for the present discussion,

$$f(e) = e(1-k_a e^2) \tag{3}$$

where $k_a$ is suitably chosen to represent the antenna characteristic. The noise $w(t)$ injected by the receiver is a white noise process having zero mean and spectral density $q$. This problem formulation is taken directly from [12]; a discussion of the approach and results in [12] vis-à-vis the current treatment is given in [13].

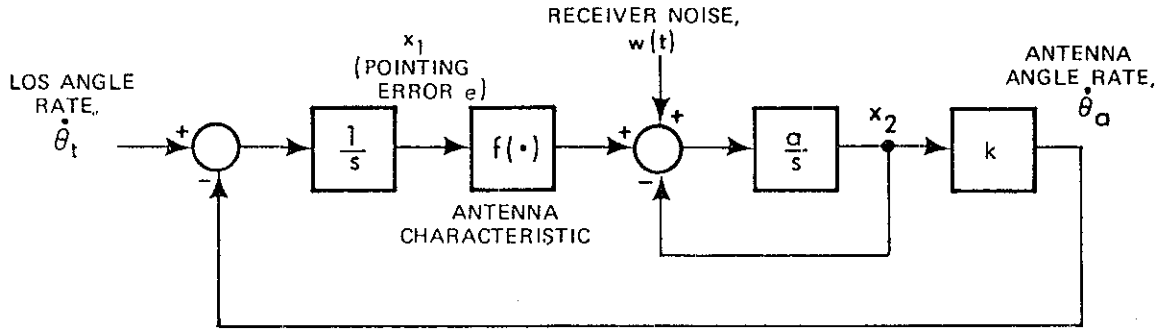


Figure 1 Antenna Pointing and Tracking Model

In a state space formulation, Fig. 1 is equivalent to

$$\dot{\underline{x}} = \underline{f}(\underline{x}) + \underline{w} \tag{4}$$

where $x_1$ is the pointing error $e$, $x_2$ is defined in Fig. 1, and

$$\underline{f}(\underline{x}) = \begin{bmatrix} -kx_2 \\ a\,(f(x_1) - x_2) \end{bmatrix} \; ; \quad \underline{w} = \begin{bmatrix} \dot{\theta}_t \\ aw(t) \end{bmatrix} \tag{5}$$

The statistics of the input $\underline{w}$ are given by

$$E\,[\underline{w}] \triangleq \underline{b} = \begin{bmatrix} \omega \\ 0 \end{bmatrix}$$

$$E\,[(\underline{w}(t)-\underline{b})(\underline{w}(\tau)-\underline{b})^T] \triangleq \overline{Q}\,\delta(t-\tau) = \begin{bmatrix} 0 & 0 \\ 0 & a^2 q \end{bmatrix} \delta(t-\tau) \tag{6}$$

The initial state statistics, assuming $x_2(0) = 0$, are

$$E[\underline{x}(0)] \triangleq \underline{m}_0 \triangleq \begin{bmatrix} m_{e_0} \\ 0 \end{bmatrix}$$

$$E[(\underline{x}(0) - \underline{m}_0)\,(\underline{x}(0) - \underline{m}_0)^T] \triangleq \overline{S}_0 \triangleq \begin{bmatrix} \sigma_{e_0}^2 & 0 \\ 0 & 0 \end{bmatrix} \tag{7}$$

where $m_{e_0}$ and $\sigma_{e_0}$ are the initial mean and standard deviation of the pointing error, respectively.

The above problem statement is in a form suitable for the application of CADET. The quasi-linear representation for $f(x_1)$ in Eq. (3) is of the form

$$f(x_1) \cong \hat{f} + n(x_1 - m_1) \tag{8}$$

where, for gaussian random variables [3], the random-input describing function components $\hat{f}$ and n are

$$\begin{aligned} \hat{f} &= m_1 - k_a(m_1^2 + 3\, s_{1,1})\, m_1 \\ n &= 1 - 3k_a(m_1^2 + s_{1,1}) \end{aligned} \tag{9}$$

and $m_1$ and $s_{1,1}$ are elements of $\underline{m}$ and $\underline{\bar{S}}$, respectively. The CADET solution is then obtained by solving Eq. (20), which specializes to

$$\begin{aligned} \dot{\underline{m}} &= \begin{bmatrix} -km_2 \\ a(\hat{f} - m_2) \end{bmatrix} + \underline{b} \\ \dot{\underline{\bar{S}}} &= \underline{\bar{N}}\,\underline{\bar{S}} + \underline{\bar{S}}\,\underline{\bar{N}}^T + \underline{\bar{Q}} \end{aligned} \tag{10}$$

subject to the initial conditions in Eq. (7), and where

$$\underline{\bar{N}} = \begin{bmatrix} 0 & -k \\ an & -a \end{bmatrix} \tag{11}$$

As noted in Appendix A, Eq. (10) is exact if $\underline{x}$ is a vector of jointly gaussian random variables; if e(0) and w(t) are gaussian and the effect of the nonlinearity is not too severe, the solution to Eq. (10) will provide a good approximation.

The solutions depicted in Fig. 2 are based on the assumption that e(0) and w(t) are gaussian. The system parameters are: $a = 50\ \text{sec}^{-1}$, $k = 10\ \text{sec}^{-1}$, $k_a = 0.4\ \text{deg}^{-2}$, $m_{e_0} = 0.4$ deg, $\sigma_{e_0} = 0.1$ deg, $q = 0.004\ \text{deg}^2$. The goal is to determine tracking capability for various values of $\omega$; for brevity, only $\omega = 4$ deg/sec is shown here. To provide a basis for assessing the accuracy of CADET, four solutions are presented. In addition to the CADET results, ensemble statistics from a 1000-trial monte carlo simulation are plotted. Solutions from [12] are also shown, labeled "linear approximation" (corresponding to $k_a = 0$) and "second-order Volterra"; the latter is based on a technique developed in [12]. The monte carlo data are depicted with 95% confidence intervals based on the gaussian assumption [1]. Evidently, the CADET solution provides a significantly better fit to the monte carlo data than either of the other analytical approximations. For higher tracking rates, $\omega \geq 6$ deg/sec, the tracking error can become so large that the antenna characteristic effectively becomes a negative gain, producing unstable solutions. This effect is predicted by CADET, whereas the linear and second-order Volterra approximations do not capture the instability [12,13].

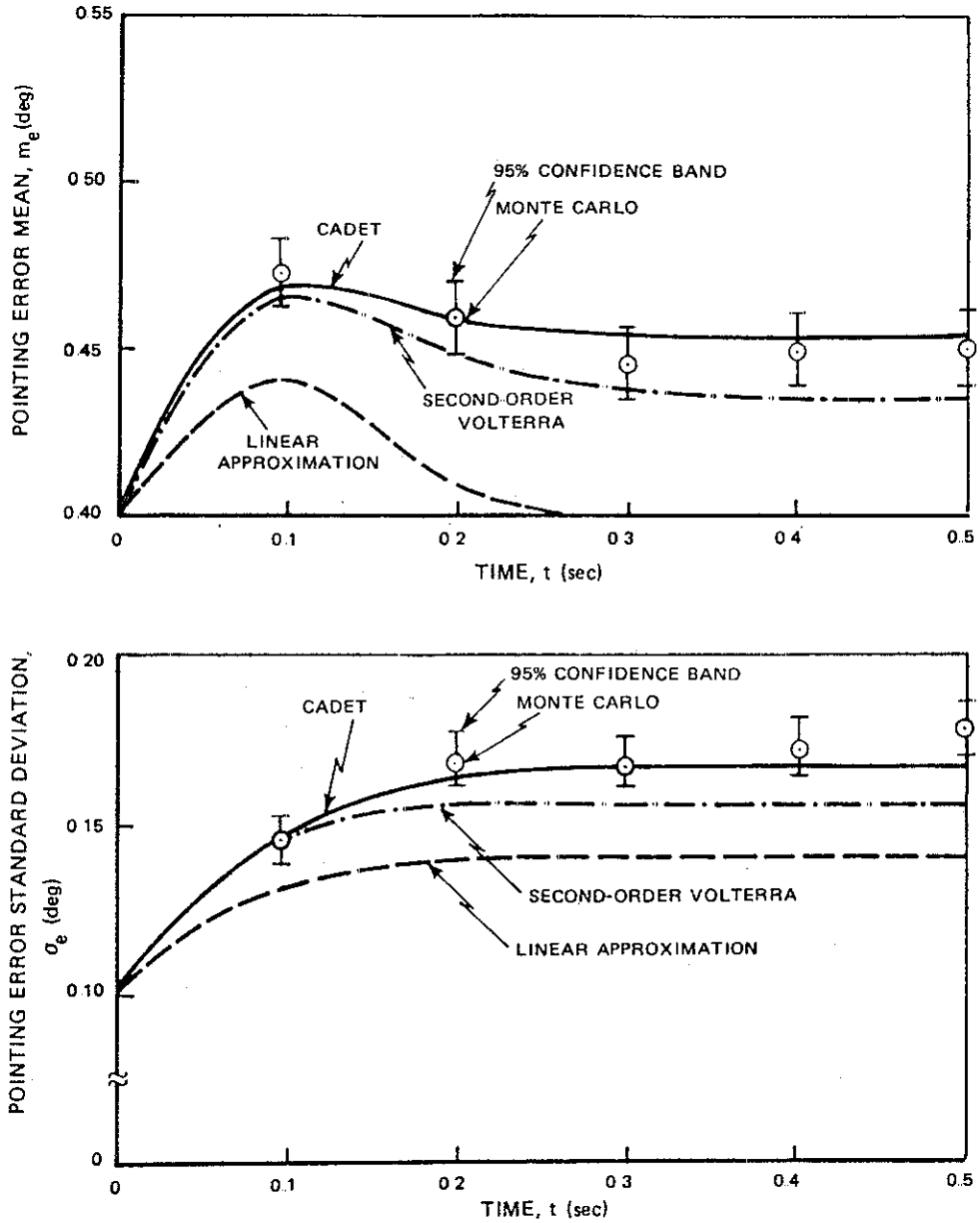


Figure 2 Pointing Error Statistics

## 2.2 PURSUER/EVADER INTERCEPT PROBLEM

Consider the problem illustrated in Figs. 3 and 4, of a pursuer and evader initially closing head-on in a plane with velocities $\underline{v}_p(0)$ and $\underline{v}_e(0)$, respectively. The evader has a random lateral acceleration, $x_4$, perpendicular to the initial line-of-sight, characterized as a first-order markov process with a standard deviation of 0.5g (16.1 ft/sec$^2$). The pursuer commanded lateral acceleration, $x_1$, is subject to saturation. The guidance command to the pursuer dynamics is given to be proportional to the line-of-sight angular rate (the so-called proportional guidance law), with the guidance gain $\alpha$ equal to 3. It is assumed that the relative closing velocity is constant, with an initial time-to-go until inter-

cept, $T_{GO}$, of 10 sec. The equations of motion corresponding to Fig. 4 can be written in the form

$$\begin{bmatrix} \dot{x}_1 \\ \dot{x}_2 \\ \dot{x}_3 \\ \dot{x}_4 \end{bmatrix} = \begin{bmatrix} -1 & \frac{\alpha}{T_{GO}^2} & \frac{\alpha}{T_{GO}} & 0 \\ 0 & 0 & 1 & 0 \\ 0 & 0 & 0 & 1 \\ 0 & 0 & 0 & -1 \end{bmatrix} \begin{bmatrix} x_1 \\ x_2 \\ x_3 \\ x_4 \end{bmatrix} + \begin{bmatrix} 0 \\ 0 \\ -f(x_1) \\ 0 \end{bmatrix} + \begin{bmatrix} 0 \\ 0 \\ 0 \\ w_4 \end{bmatrix} \qquad (12)$$

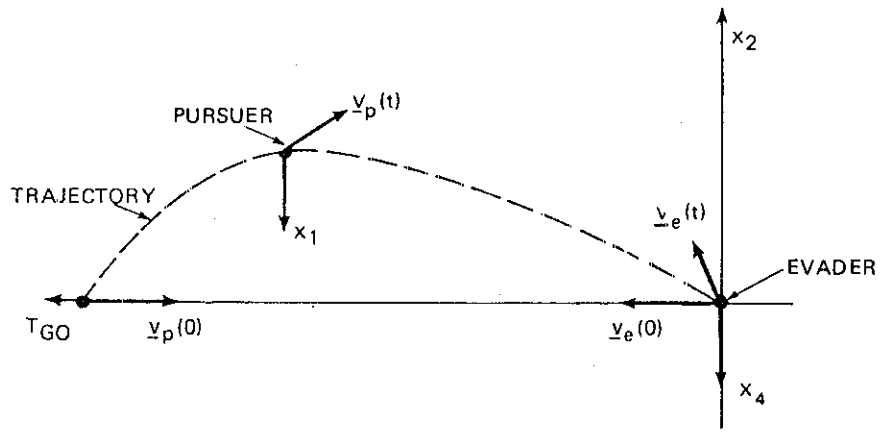


Figure 3 Pursuer/Evader Geometry

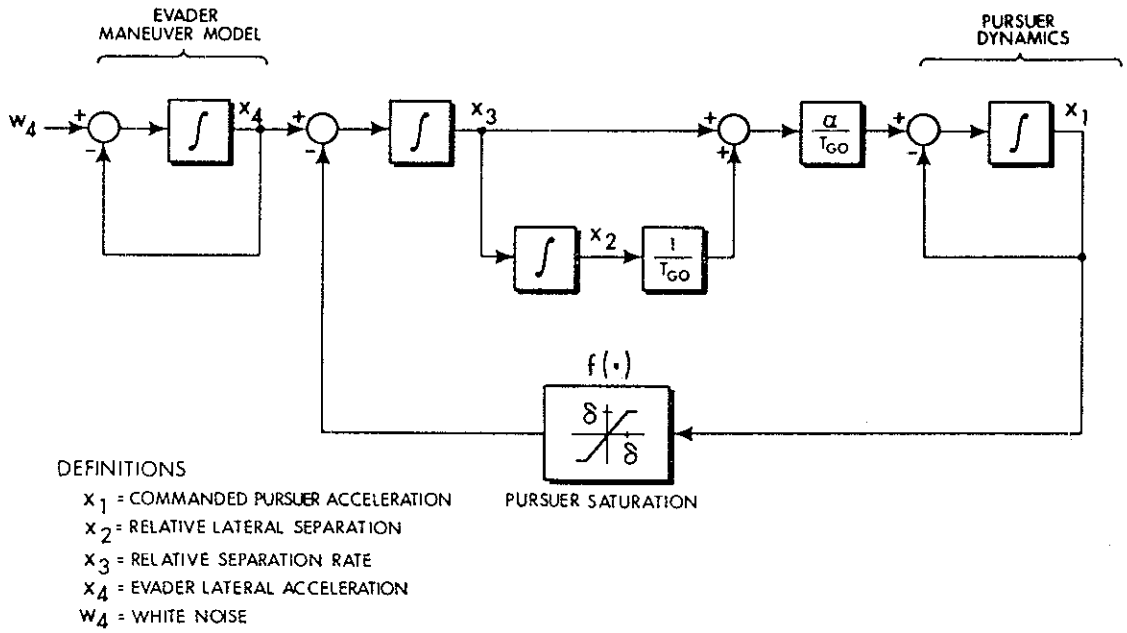


Figure 4 Kinematic Guidance Loop With Pursuer Lateral Acceleration Saturation

Recognizing that the mean state vector is zero in this example, the covariance equation (Eq. (20)) is formed from Eq. (12) with $f(x_1)$ replaced by the random-input describing function gain associated with the saturation element. Assuming $x_1$ to be gaussian with zero mean and standard deviation $\sigma_{x_1}$, the describing function is [3]

$$n = 2\ \mathrm{PI}\ (\delta/\sigma_{x_1}) - 1$$

$$= \sqrt{\frac{2}{\pi}} \int_{-\infty}^{\delta/\sigma_{x_1}} \exp(-y^2/2)\ dy - 1 \qquad (13)$$

where PI represents the standard probability intergral. Solutions to the covariance equation for the root-mean-square (rms) values of the lateral separation for two different pursuer acceleration saturation limits are plotted as functions of time in Fig. 5. Results from a 200-trial monte carlo analysis are also presented for comparison. At t = 10 sec (or $T_{GO} = 0$), the lateral separation represents the intercept miss distance.

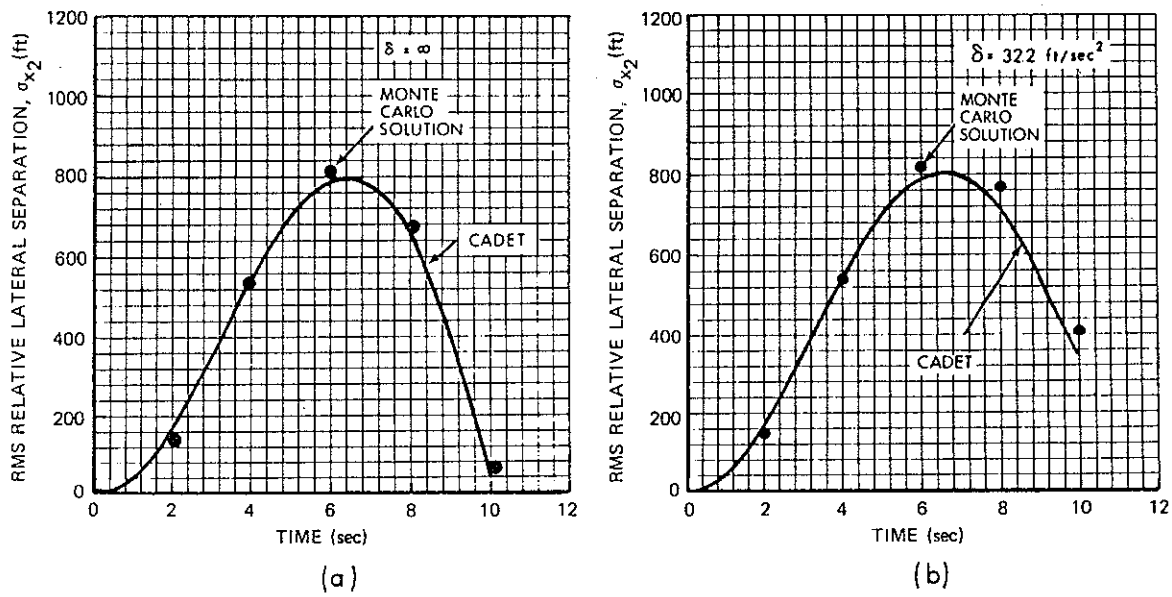


Figure 5 Simulation Results for Two Levels of Pursuer Lateral Acceleration Saturation

In Fig. 5(a), the equations of motion are linear, since $\delta = \infty$; thus, the CADEI results are exact. In this case, the close agreement with the monte carlo data is a measure of the accuracy of the monte carlo analysis. In Fig. 5(b), good agreement between monte carlo and CADEI is maintained even though the equations contain a significant nonlinearity that has substantially degraded the performance of the pursuer.

This is the simplest example of a wide variety of intercept problems that have been treated by CADEI. Further examples, of higher order (more than 20 states) and having many nonlinearities (more than 20), may be found in [9] and [10].

## 2.3 SPACECRAFT SPIN-UP PROBLEM

Figure 6 portrays the nose cone of a spacecraft having thrusters mounted on the cone base. The thrusters are ignited after injection into orbit, yielding thrusts $T_1$ and $T_2$ which spin-up the nose cone to achieve spin stabilization. Because of asymmetries in the vehicle mass distribution and imperfect thrust application, the spinning motion about the x-axis will be accompanied by a coning motion of the x-axis (assumed to be a principal body axis) about the angular momentum vector. This example illustrates how CADET can be used to compute the coning angle statistics as a function of the vehicle configuration, initial condition statistics, and thrust statistics.

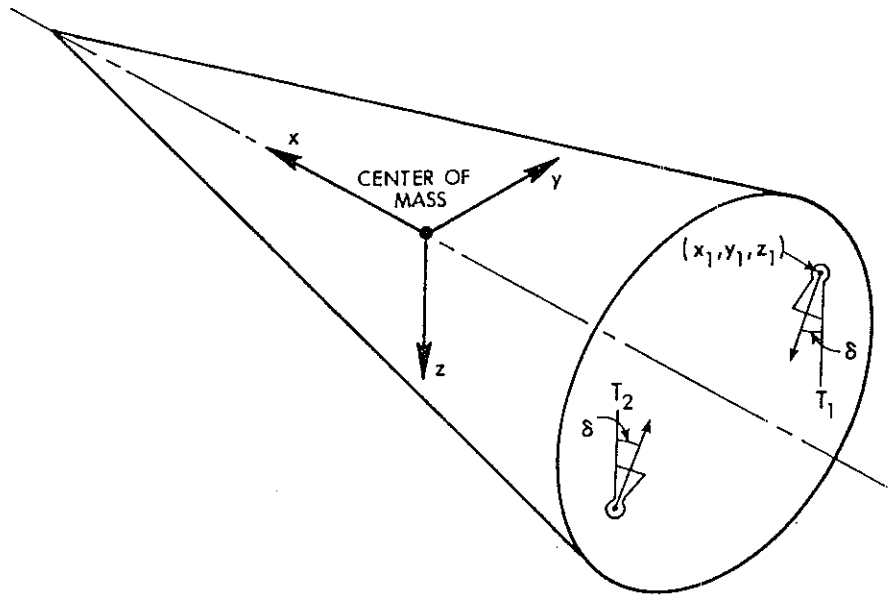


Figure 6 Spacecraft Nose Cone Geometry

It is assumed that the body x, y, and z axes are principal axes, the thrusters are symmetrically placed with respect to the vehicle x-axis, and the thrust vectors lie in the plane of the cone base. Under these conditions, the equations of motion for the components of vehicle angular velocity in body axes are

$$\begin{aligned}
\dot{\omega}_x &= \frac{1}{I_x}\left[(T_1+T_2)(y_1\cos\delta + z_1\sin\delta) + (I_y-I_z)\omega_y\omega_z\right] \\
\dot{\omega}_y &= \frac{1}{I_y}\left[(T_2-T_1)x_1\cos\delta + (I_z-I_x)\omega_x\omega_z\right] \\
\dot{\omega}_z &= \frac{1}{I_z}\left[(T_2-T_1)x_1\sin\delta + (I_x-I_y)\omega_x\omega_y\right]
\end{aligned} \tag{14}$$

where $x_1$, $y_1$, $z_1$ are the coordinates of thruster $I_1$ in Fig. 7; $\omega_x$, $\omega_y$, $\omega_z$ denote components of angular velocity; $I_x$, $I_y$, $I_z$ denote moments of inertia about body axes; and $\delta$ is the thruster pointing angle defined in Fig. 6. The coning angle $\theta_c$ is given by the relation

$$\theta_c = \sin^{-1}\sqrt{\frac{I_y^2\omega_y^2 + I_z^2\omega_z^2}{I_x^2\omega_x^2 + I_y^2\omega_y^2 + I_z^2\omega_z^2}} \simeq \frac{\sqrt{I_y^2\omega_y^2 + I_z^2\omega_z^2}}{I_x\omega_x} \qquad (15)$$

where $\theta_c$ is assumed to be a small angle. The angular velocities and thrust levels at the beginning of spin-up are assumed to be independent gaussian random variables.

Space does not permit a detailed presentation of the CADEI model corresponding to Eqs. (14) and (15). The model is obtained by straightforward application of Eqs. (18) and (20) after linearizing $\theta_c$ in Eq. (15) about the mean of $\omega_x$ and the random components of $\omega_y$ and $\omega_z$. The nonlinearities which are quasi-linearized in this model are the angular velocity cross products, $\omega_y\omega_z$, etc.; describing functions are directly derivable from Eq. (28). Figure 7 presents monte carlo-CADEI comparisons of the rms coning angle as a function of time (referenced to the start of spin-up). Both cases have the following initial condition and parameter values:

$$E[\omega_x(0)] = E[\omega_y(0)] = E[\omega_z(0)] = 0$$

$$E[\omega_x^2(0)] = 5.61 \times 10^{-5} \text{ rad}^2/\text{sec}^2$$

$$E[\omega_y^2(0)] = E[\omega_z^2(0)] = 3.06 \times 10^{-4} \text{ rad}^2/\text{sec}^2 \qquad (16)$$

$$\delta = 26 \text{ deg}, \; x_1 = -0.81 \text{ m}, \; y_1 = 0.18 \text{ m}, \; z_1 = 0.0547 \text{ m}$$

$$I_x = 1.84 \text{ kg}\cdot\text{m}^2, \; E[T_1] = E[T_2] = 11.2 \text{ N}$$

$$E[(T_1 - 11.2)^2] = E[(T_2 - 11.2)^2] = 0.0126 \text{ N}^2$$

In Case A, the moments of inertia about the y and z axes are equal; this condition, together with the chosen set of initial conditions, implies that $\omega_x$ has a

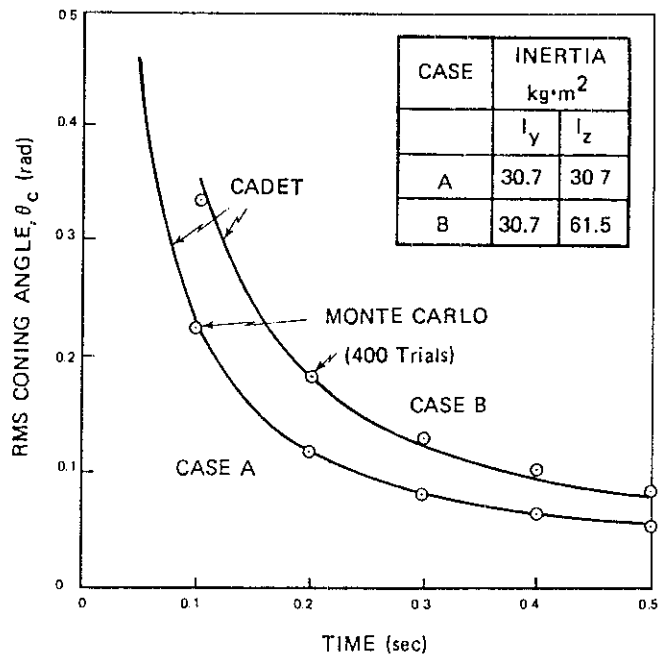


Figure 7 RMS Coning Angle Time-History

deterministic solution. Consequently, the CADEI model for Eq. (14) is linear; the only nonlinearity is the expression for the coning angle. However, in Case B, the x and y moments of inertia are unequal, resulting in a nonlinear model for Eq. (14) which is quasi-linearized in the CADEI analysis.

Figure 7 shows excellent agreement between monte carlo and CADEI results for both cases. The best agreement is obtained for Case A, which has the lesser degree of nonlinearity; however, the CADEI result is also quite accurate in Case B.

## 3. SUMMARY OF CADET CAPABILITIES

One of the main arguments advanced for the use of CADEI in obtaining projections of nonlinear system performance is the significant reduction in computer central processing unit (CPU) time achieved by using CADET instead of the monte carlo method. In making this comparison, the number of monte carlo trials that must be performed in order to obtain acceptably accurate results must be established.

To achieve $\pm$ 10% accuracy with 95% confidence, 256 monte carlo trials are needed in the gaussian case*. This level of accuracy appears to be reasonable for many applications; hence, the 256-trial set is chosen as the standard. The accuracy of CADEI is typically found to be competitive with 256 monte carlo trials, in the sense that the CADET results lie within the 95% confidence bands for the monte carlo results. CADEI has demonstrated up to 30:1 CPU time advantage over 256-trial monte carlo sets in applications having more than 40 state variables and up to 26 nonlinearities. In pursuer/evader studies, such effects as nonlinear airframe characteristics, seeker gimbal mass imbalance and coulomb friction, nonlinear springs, coordinate transformations, and nonlinear kinematics have been treated. This accumulated experience clearly demonstrates the advantages of CADEI as an analysis tool for nonlinear stochastic systems.

## APPENDIX A - THE COVARIANCE ANALYSIS DESCRIBING FUNCTION TECHNIQUE (CADEI)

The Covariance Analysis Describing Function Technique (CADEI) is a method for directly determining the statistical properties of solutions of nonlinear systems with random inputs [8]. The principal advantage of this technique is that it greatly reduces the need for monte carlo simulation, thereby achieving substantial savings in computer data processing time.

The dynamics of a nonlinear continuous-time stochastic system can be represented by a first-order vector differential equation in which $\underline{x}(t)$ is the system state vector and $\underline{w}(t)$ is a forcing function vector,

$$\dot{\underline{x}}(t) = \underline{f}(\underline{x},t) + \overline{G}(t)\ \underline{w}(t) \qquad (17)$$

The state vector is composed of any set of variables sufficient to describe the behavior of the system completely. The forcing function vector $\underline{w}(t)$ represents disturbances as well as control inputs that may act upon the system. In what follows, $\underline{w}(t)$ is assumed to be composed of a mean or deterministic value $\underline{b}(t)$ and a random component $\underline{u}(t)$, the latter being comprised of elements which are

* If nonlinearity causes an appreciable departure from the gaussian case, more trials may be needed for $\pm$ 10% accuracy [1].

uncorrelated in time; that is, $\underline{u}(t)$ is a white noise process having the spectral density matrix $\bar{Q}(t)$. Similarly, the state vector has a deterministic component $\underline{m}(t)$ and a random part $\underline{r}(t)$; for simplicity, $\underline{m}(t)$ will usually be called the mean vector. Thus the state vector $\underline{x}(t)$ is described statistically by its mean vector and covariance matrix, $\bar{S}(t)$. Henceforth, the time dependence of the variables $\underline{w}$, $\underline{b}$, $\underline{u}$, $\bar{Q}$, $\underline{x}$, $\underline{m}$, $\underline{r}$, and $\bar{S}$ will not be explicitly denoted by (t).

The differential equations that govern the propagation of the mean vector and covariance matrix for the system described by Eq. (17) can be derived directly, as demonstrated in [14], to be

$$\begin{aligned} \dot{\underline{m}} &= E\,[\underline{f}(\underline{x},t)] + \bar{G}(t)\underline{b} \\ &\triangleq \hat{\underline{f}} + \bar{G}(t)\underline{b} \\ \dot{\bar{S}} &= E\,[\underline{f}\,\underline{r}^T] + E\,[\underline{r}\,\underline{f}^T] + \bar{G}(t)\bar{Q}\,\bar{G}^T(t) \end{aligned} \tag{18}$$

The equation for $\bar{S}$ can be put into a form analogous to the covariance equations corresponding to $\underline{f}$ being linear, by defining the auxiliary matrix N through the relationship

$$\bar{N}\,\bar{S} \triangleq E\,[\underline{f}(\underline{x},t)\;\underline{r}^T] \tag{19}$$

Then Eq. (18) may be written as

$$\begin{aligned} \dot{\underline{m}} &= \hat{\underline{f}} + \bar{G}(t)\underline{b} \\ \dot{\bar{S}} &= \bar{N}\,\bar{S} + \bar{S}\,\bar{N}^T + \bar{G}(t)\bar{Q}\,\bar{G}^T(t) \end{aligned} \tag{20}$$

The quantities $\hat{\underline{f}}$ and $\bar{N}$ defined in Eqs. (18) and (19) must be determined before one can proceed to solve Eq. (20). Evaluating the indicated expected values requires knowledge of the joint probability density function (joint pdf) of the state variables. While it is possible, in principle, to evolve the n-dimensional joint pdf $p(\underline{x},t)$ for a nonlinear system with random inputs by solving a set of partial differential equations known as the Fokker-Planck equation or the forward equation of Kolmogorov [14], this procedure is generally not feasible from a practical point of view. The fact that the pdf is not available precludes the exact solution of Eq. (20).

One procedure for obtaining an approximate solution to Eq. (20) is to assume the form of the joint probability density function of the state variables in order to evaluate $\hat{\underline{f}}$ and $\bar{N}$ according to Eqs. (18) and (19). Although it is possible to use any joint pdf, all CADEI development to date has been based on the assumption that the state variables are jointly normal; the choice was made because it is both reasonable and convenient.

While the above assumption is strictly true only for linear systems driven by gaussian inputs, it is often approximately valid in nonlinear systems with nongaussian inputs. Although the output of a nonlinearity with a gaussian input is generally nongaussian, it is known from the central limit theorem [15] that random processes tend to be made gaussian when passed through low-pass linear

dynamics ("filtered"). Thus, in many instances, one may rely on the linear part of the system to insure that nongaussian nonlinearity outputs result in nearly gaussian system variables as signals propagate through the system. By the same token, if there are nongaussian system inputs which are passed through low-pass linear dynamics, the central limit theorem can again be invoked to justify the assumption that the state variables are approximately jointly normal. The validity of the gaussian assumption for nonlinear systems with gaussian inputs has been studied and verified for a wide variety of systems.

From a pragmatic viewpoint, the gaussian hypothesis serves to simplify the mechanization of Eq. (20) significantly by permitting each scalar nonlinear relation in $\underline{f}(\underline{x},t)$ to be treated in isolation [8], with $\hat{\underline{f}}$ and $\overline{\underline{N}}$ formed from the individual random-input describing functions (RIDF's) for each nonlinearity. It is this direct connection with describing function theory that has motivated the name, Covariance Analysis Describing Function Technique (CADET). Since RIDF's have been catalogued for numerous single-input nonlinearities [3,4] and are readily available for many multi-input nonlinearities (see Appendix B), the implementation of CADET is a straightforward procedure for the analysis of many nonlinear systems. This method of dealing with nonlinear effects in stochastic systems, also called quasi-linearization or statistical linearization, is discussed in [5] as well.

As a consequence of the gaussian assumption, the random-input describing functions for a given nonlinearity are dependent only upon the mean and the covariance of the system state vector. Thus, $\hat{\underline{f}}$ and $\overline{\underline{N}}$ are written explicitly as

$$\begin{aligned} \hat{\underline{f}} &= \hat{\underline{f}}(\underline{m},\underline{S},t) \\ \overline{\underline{N}} &= \overline{\underline{N}}(\underline{m},\underline{S},t) \end{aligned} \tag{21}$$

Furthermore, it can be proved [6, 7] that

$$\overline{\underline{N}}(\underline{m},\underline{S},t) = \frac{d}{d\underline{m}}\,\hat{\underline{f}} \tag{22}$$

Since calculating $\hat{\underline{f}}$ is required for the propagation of the mean (Eq. (20)), it is generally much easier to employ Eq. (22) than to evaluate $\overline{\underline{N}}$ directly using Eq. (19).

Relations of the form indicated in Eq. (21) permit the direct evaluation of $\hat{\underline{f}}$ and $\overline{\underline{N}}$ at each integration step in the propagation of $\underline{m}$ and $\underline{S}$. Note that the dependence of $\hat{\underline{f}}$ and $\overline{\underline{N}}$ on the statistics of the state vector is due to the existence of nonlinearities in the system.

A comparison of quasi-linearization with the classical Taylor series or small signal linearization technique provides a great deal of insight into the success of the RIDF in capturing the essence of nonlinear effects. Figure 8 illustrates this comparison with a concrete example. If a saturation or limiter is present in a system and its input x is zero-mean, the Taylor series approach leads to replacing f(x) with a unity gain regardless of the input amplitude,

while quasi-linearization gives rise to a gain that decreases as the rms value of x, $\sigma_x$, increases. The latter approximate representation of f(x) much more accurately reflects the nonlinear effect; in fact, the saturation is completely neglected in the small-signal linear model, so it would not be possible to determine its impact. The fact that RIDF's retain an essential characteristic of system nonlinearities -- input-amplitude dependence -- provides the basis for the proven accuracy of CADET.

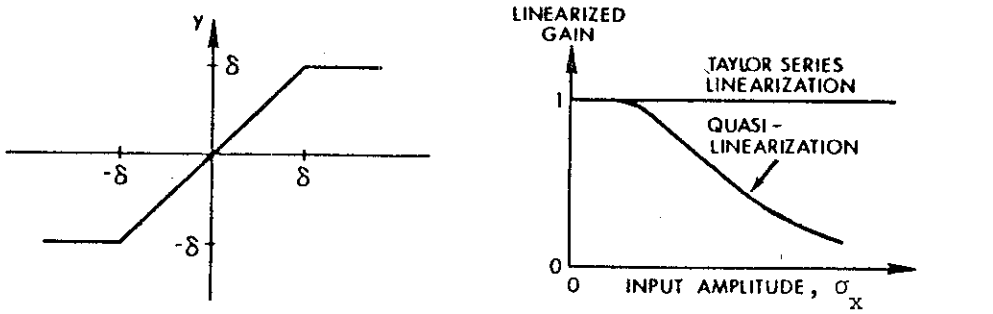


(a) NONLINEAR FUNCTION (IDEAL LIMITER)

(b) TAYLOR SERIES AND QUASI-LINEARIZED GAINS (m = 0)

Figure 8 Illustration of a Describing Function Representation

APPENDIX B - PRACTICAL RIDF EVALUATION TECHNIQUES

References [3,4] catalog RIDF's for a wide variety of single-input nonlinearities. Since CADET has proven to be useful in treating more complicated nonlinear effects -- modeled by multi-input nonlinearities -- a few approaches for treating functions of several variables are outlined in this appendix.

In general, for the single multi-input nonlinearity $f(\underline{v})$ where $\underline{v}$ is a vector of jointly gaussian inputs with statistics

$$E[\underline{v}] = \underline{m}_v \triangleq [m_i]$$
$$E[(\underline{v}-\underline{m}_v)(\underline{v}-\underline{m}_v)^T] = \underline{S}_v \triangleq [s_{i,j}] \tag{23}$$

the RIDF representation is

$$f \cong \hat{f} + \underline{n}^T(\underline{v}-\underline{m}_v) \tag{24}$$

where the RIDF components $\hat{f}$ and $\underline{n}$ are [11]

$$\hat{f} = \frac{1}{\sqrt{(2\pi)^n |\underline{S}_v|}} \int_{-\infty}^{\infty}\int \cdots f(\underline{v}) \exp\left(-1/2\ (\underline{v}-\underline{m}_v)^T\ \underline{S}_v^{-1}(\underline{v}-\underline{m}_v)\right) dv_1\ dv_2 \cdots \tag{25}$$

and

$$\underline{n}^T = \frac{\partial f}{\partial \underline{m}_v} \tag{26}$$

Exact analytic results for several broad classes of multi-input nonlinearities are derived in [11]. These can be outlined as follows:

Case 1: $$f(v_1,v_2) = v_1\ g(v_2) \tag{27}$$

yields

$$\hat{f} = m_1 \hat{g} + s_{1,2} n_g$$

$$\underline{n} = \begin{bmatrix} \hat{g} \\ m_1 n_g + s_{1,2} \dfrac{\partial n_g}{\partial m_2} \end{bmatrix} \tag{28}$$

where $\hat{g}$ and $n_g$ are the RIDF constituents of g,

$$g \cong \hat{g} + n_g (v_2 - m_2) \tag{29}$$

Case 2:
$$f(v_1, v_2) = v_1^k \, g(v_2) \tag{30}$$

yields

$$\hat{f} = \sum_{j=0}^{k} \binom{k}{j} s_{1,2}^j \, E[v_1^{k-j}] \, \frac{\partial^j \hat{g}}{\partial m_2^j} \tag{31}$$

where $\binom{k}{j}$ is the standard binomial coefficient, $k(k-1)\ldots(k-j+1)/j!$ The formula for $\underline{n}$ is obtained directly by partial differentiation (Eq. (26)).

Case 3:
$$f(v_1, v_2, v_3) = v_1 \, g(v_2, v_3) \tag{32}$$

yields

$$\hat{f} = m_1 \hat{g} + s_{1,2} n_{g_2} + s_{1,3} n_{g_3} \tag{33}$$

Results of the sort illustrated in this paragraph reduce RIDF evaluation from a tedious procedure of multiple integrations (Eq. (25)) to a straightforward substitution, for a number of nonlinearity forms.

Two approximate techniques are widely useful when analytic results are not available. The first involves series expansions of the nonlinearity, and the second is direct numerical integration. In both cases, only the evaluation of $\hat{f}$ is considered (Eq. (25)) since $\underline{n}$ follows directly. For simplicity, only functions of two random variables are considered in illustrations.

A Taylor series expansion of $f(\underline{v})$ about the mean leads to

$$f(\underline{v}) = f(\underline{m}) + \frac{\partial f(\underline{m})}{\partial \underline{m}} (\underline{v} - \underline{m}) + \frac{1}{2} (\underline{v} - \underline{m})^T \left[ \frac{\partial^2 f(\underline{m})}{\partial m_i \partial m_j} \right] (\underline{v} - \underline{m}) + \ldots \tag{34}$$

Taking the expected value term-by-term yields, e.g.,

$$\hat{f} = f(\underline{m}) + \frac{1}{2} \left[ s_{1,1} \frac{\partial^2 f}{\partial m_1^2} + 2 \, s_{1,2} \frac{\partial^2 f}{\partial m_1 \partial m_2} + s_{2,2} \frac{\partial^2 f}{\partial m_2^2} \right] + \ldots \tag{35}$$

Often, truncating the series at the second-order terms as shown in Eq. (35) results in a good approximate RIDF, especially if the value of $\underline{m}$ is not near a singularity of $f(\underline{v})$. More terms can be included if greater accuracy is required.

Numerical integration is most simply implemented by using a transformation

$$\underline{u} = \overline{\overline{T}}(\underline{v} - \underline{m}) \tag{36}$$

which leads to a $\underline{u}$-vector with an identity covariance matrix ($\overline{\overline{S}}_u = \overline{\overline{I}}$); a grid of points in the $\underline{u}$-space can then be established, and summation over the grid approximates the integral in Eq. (25). For example, with $n_r \times n_\phi$ cells as shown in Fig. 9, and with weighting

$$w_j = \frac{1}{\sqrt{2\pi}} \exp\left(-\frac{1}{2}\left(j - \frac{1}{2}\right)^2 \Delta r^2\right) \tag{37}$$

the approximation is

$$\hat{f} \cong \sum_{j=1}^{n_r} w_j \sum_{k=1}^{n_\phi} f(\underline{v}(u_{1,j,k}, u_{2,j,k})) \tag{38}$$

where

$$u_{1,j,k} = \left(j - \frac{1}{2}\right)\Delta r \cos(\phi_k)$$

$$u_{2,j,k} = \left(j - \frac{1}{2}\right)\Delta r \sin(\phi_k)$$

$$\phi_k = 2\pi(k-1)/n_\phi \tag{39}$$

and $\underline{v}$ is found by inverting Eq. (36). If the nonlinearity is well-behaved so that a very fine grid is not needed, and if efficient coding is used, the computational burden of direct numerical integration is not prohibitive; any degree of accuracy is possible with a corresponding trade-off in computer time.

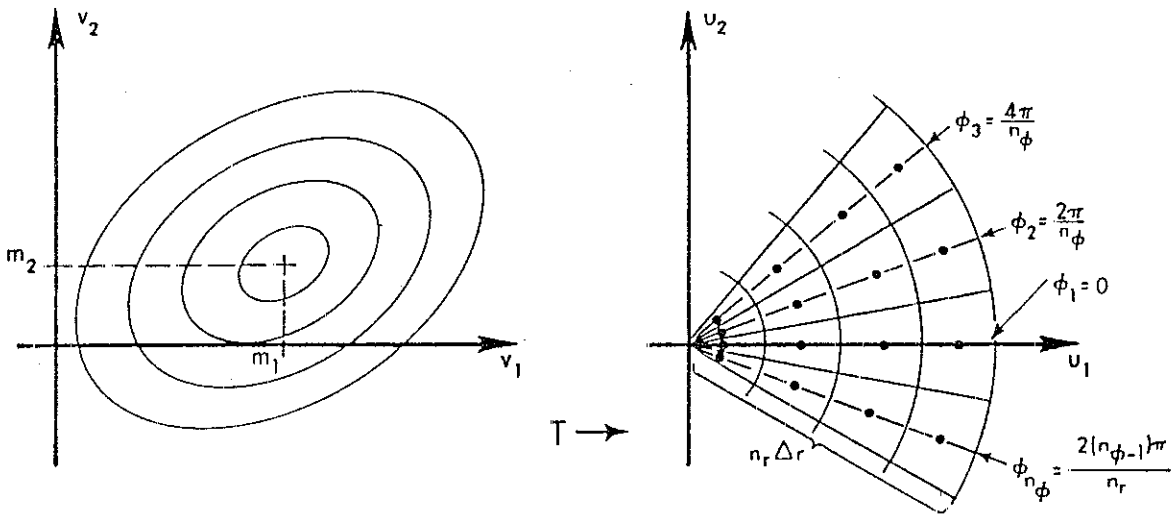


Figure 9. Transformation of Variables for Numerical Integration of Random-Input Describing Functions

The availability of RIDF's for the large number of single-input nonlinearities treated in [3,4], augmented by the approaches for multi-input nonlinearities outlined in this appendix, permit the routine application of CADET to a wide variety of complicated, highly nonlinear problems.

REFERENCES


1. Taylor, J. H., "On the Credibility of the Monte Carlo Method for Nonlinear Systems Analysis," Tenth Annual Pittsburgh Modeling and Simulation Conference, Pittsburgh, Pennsylvania, April 1979.
2. Gelb, A. (Ed.), Applied Optimal Estimation, MIT Press, Cambridge, Mass., 1974.
3. Gelb, A. and Vander Velde, W. E., Multiple-Input Describing Functions and Nonlinear System Design, McGraw-Hill Book Co., New York, 1968.
4. Atherton, D. P., Nonlinear Control Engineering, Van Nostrand Reinhold Co., London, 1975.
5. Hedrick, J. K. and Paynter, H. M. (Eds.), Nonlinear System Analysis and Synthesis: Vol. 1 – Fundamental Principles, American Society of Mechanical Engineers, New York, 1978.
6. Kazakov, I. E., "Generalization of the Method of Statistical Linearization to Multidimensional Systems," Avtomatika i Telemekhanika, Vol. 26, No. 7, July 1965, pp. 1210-1215.
7. Phaneuf, R. J., "Approximate Nonlinear Estimation," Ph.D. Thesis, Dept. of Aeronautics and Astronautics, M.I.T., Cambridge, Mass., May 1968.
8. Gelb, A. and Warren, R. S., "Direct Statistical Analysis of Nonlinear Systems: CADET," AIAA Journal, Vol. 11, No. 5, May 1973, pp. 689-694.
9. Warren, R. S., Price, C. F., Gelb, A., and Vander Velde, W. E., "Direct Statistical Evaluation of Nonlinear Guidance Systems," AIAA Guidance and Control Conference, Key Biscayne, Florida, August 1973.
10. Taylor, J. H. and Price, C. F., "Statistical Analysis of Nonlinear Systems Performance via CADET$^{TM}$," Sixth Annual Southeastern Symposium on System Theory, Baton Rouge, Louisiana, February 1974.
11. Taylor, J. H., "Random-Input Describing Functions for Multi-Input Nonlinearities," Int. J. of Control, Vol. 23, No. 2, February 1976, pp. 277-281.
12. Landau, M. and Leondes, C. T., "Volterra Series Synthesis of Nonlinear and Stochastic Tracking Systems," IEEE Trans. on Aerospace and Electronic Systems, Vol. AES-11, No. 2, March 1975, pp. 245-265.
13. Taylor, J. H., "Comment on 'Volterra Series Synthesis of Nonlinear Stochastic Tracking Systems'," IEEE Trans. on Aerospace and Electronic Systems, Vol. AES-14, No. 2, March 1978, pp. 390-393.
14. Jazwinski, A. H., Stochastic Processes and Filtering Theory, Academic Press, New York, 1970.
15. Papoulis, A., Probability, Random Variables, and Stochastic Processes, McGraw-Hill Book Co., New York, 1965.